GEOPHYSICAL RESEARCH LETTERS, VOL. 33, L15309, doi:10.1029/2006GL026414, 2006

A shock-tube investigation of the dynamics of gas-particle mixtures: Implications for explosive volcanic eruptions

K. Chojnicki,[1] A. B. Clarke,[1] and J. C. Phillips[2]

Received 24 March 2006; revised 22 May 2006; accepted 13 June 2006; published 8 August 2006.

[1] We use 1-D shock-tube experiments to investigate the dynamics of rapidly-decompressed gas-particle mixtures and associated shock waves, with application to the initial stages of Vulcanian and Plinian eruptions. For particle sizes 45–150 μm and pressure ratios 1–70, experimental particle Reynolds numbers reach 10^4 and impulsive accelerations reach 150 g. The experiments suggest that particles hinder gas motion via an interphase drag force, reducing shock strength and velocity. Gas-particle mixture velocities decrease with increasing particle diameter for a given initial pressure ratio and are less than those predicted by pseudogas approximations and existing interphase drag relationships due to imperfect phase coupling and unsteady flow during high-acceleration stages. We present a new analysis for predicting shock strength and velocity for gas-particle mixtures, and apply our improved interphase drag terms to the high-acceleration, eruption initiation stage of Vulcanian eruptions. **Citation:** Chojnicki, K., A. B. Clarke, and J. C. Phillips (2006), A shock-tube investigation of the dynamics of gas-particle mixtures: Implications for explosive volcanic eruptions, *Geophys. Res. Lett.*, *33*, L15309, doi:10.1029/2006GL026414.

1. Introduction

[2] High-speed gas-particle flows result from explosive volcanic activity in the form of stratospheric scale Plinian eruptions, smaller scale Vulcanian explosions, and pyroclastic flows. In this paper, we use 1-D shock tube experiments [after *Anilkumar et al.*, 1993; *Cagnoli et al.*, 2002] to understand the behavior of rapidly-decompressed gas-particle mixtures and associated shock waves. Gas-particle mixtures from explosive volcanic flows are commonly approximated as a single, perfectly-coupled fluid, or pseudogas, whose bulk properties are described as simple functions of gas volume fraction [e.g., *Wallis*, 1969; *Wilson et al.*, 1980; *Kieffer*, 1981; *Melnik et al.*, 2005]. This approach is not realistic for all eruptive conditions, so interphase drag relationships have been used to account for slip between gas and particles [e.g., *Valentine and Wohletz*, 1989; *Dobran et al.*, 1993; *Neri and Macedonio*, 1996]. However, these are typically derived from steady-state experiments [e.g., *Ergun*, 1952], which seem to be inappropriate for high accelerations associated with eruption initiation. Understanding the dynamics of rapidly accelerating gas-particle mixtures and their interaction with shock waves is important for testing explosive eruption models, and for interpretation of microbarograph measurements of pressure waves at active volcanoes [*Ishihara*, 1985; *Morrissey and Chouet*, 1997; *Johnson et al.*, 2003].

[3] After introducing shock-tube theory and describing our experimental methods (sections 2 and 3), we compare our laboratory results with existing pseudogas and interphase drag relationships (sections 4 and 5). We then present a new analysis of the behavior of rapidly decompressed gas-particle mixtures, yielding new interphase drag relationships, and discuss implications for shock wave characteristics and gas-particle mixture acceleration (section 5). We then apply our findings to typical Vulcanian eruptions (section 6).

2. Background

[4] The classical shock tube consists of a high-pressure gas (driver section) separated from a low-pressure gas (expansion section) by a diaphragm (Figure 1a; after *Saad*, 1985). Instantaneous rupture of the diaphragm forms a normal shock wave that travels at supersonic speed through the expansion section, while rarefaction waves travel into the driver section at the sound speed of the driver gas [*Saad*, 1985]. The initial pressures in the driver and expansion sections are p_4 and p_1, respectively, and the pressure behind the shock is p_2. The shock strength $\frac{p_2}{p_1}$ for inviscid flow is

$$\frac{p_2}{p_1} = 1 + \frac{2\gamma}{\gamma + 1}\left(M_s^2 - 1\right) \tag{1}$$

where M_s is the shock Mach number (the ratio of the shock speed to the sound speed, c, of the expansion section gas), and γ is the ratio of specific heats for the gas, (Figure 1a and 1b). The gas velocity behind the shock is [*Saad*, 1985]

$$u_2 = \frac{c_1}{\gamma_1}\left(\frac{p_2}{p_1} - 1\right)\sqrt{\frac{\frac{2\gamma_1}{\gamma_1+1}}{\left(\frac{p_2}{p_1}\right) + \left(\frac{\gamma_1-1}{\gamma_1+1}\right)}}. \tag{2}$$

3. Experimental Method

[5] In 1-D shock tube experiments, monodisperse mixtures of Ballotini glass spheres (Potters Inc.) and interstitial air were rapidly decompressed. The spheres were loaded into the high-pressure test section at atmospheric pressure (Figure 1c), with gas volume fractions α between 0.40–0.47. A plastic diaphragm was placed between the driver and expansion sections, and the expansion section was pumped down to vacuum pressures. A Redlake high-speed

[1]School of Earth and Space Exploration, Arizona State University, Tempe, Arizona, USA.
[2]Centre for Environmental and Geophysical Flows, Department of Earth Sciences, University of Bristol, Bristol, UK.

0094-8276/06/2006GL026414$05.00

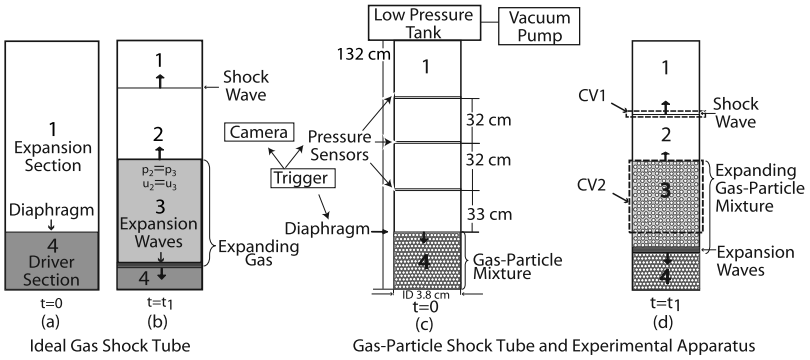

Figure 1. Shock tube schematics.

video camera (250–500 fps) and piezo-electric pressure sensors (PCB Inc., sampling at 100 kHz) were triggered simultaneously with diaphragm rupture, to measure mixture and shock velocities. The pressure ratio across the diaphragm p_4/p_1 was varied from 1–70 for each of three particle sizes 45, 90 and 150 μm. Further experiments with small (4 cm) and large (12 cm) gaps between the diaphragm and the top of a bed of 45 μm particles were performed to determine the sensitivity of the flow dynamics to gap spacing. Shock strength was calculated directly as the ratio of pressures on either side of the shock (identified in the pressure transducer data as a sharp, significant increase in pressure). Shock velocities were determined using the known distance between pressure sensors (32 cm) and the difference in the arrival times of the shock at each sensor. High-speed videography was used to track the mixture flow front. As observed by *Cagnoli et al.* [2002], some of the flow fronts were irregular adding a small unsystematic error to the mixture velocity.

4. Experimental Results

[6] Figure 2 shows the relationship between p_4/p_1 and the velocity (Figure 2a) and strength (Figure 2b) of the shock generated by the decompression experiments. The shock strengths and velocities in the experiments with air only (no particles) on both sides of the diaphragm (open triangles) generally agree with values predicted by 1-D shock tube theory (solid line; equation (1)) for air at a sound speed of 330 m s^{-1}, appropriate for our laboratory conditions.

[7] The presence of particles in the experiments (squares, dots, open circles) reduces shock velocities by approximately 30–40% and strengths by almost 60% compared to the air experiments. There is no obvious correlation between particle size and shock velocity or strength, with all particle-size data forming a single trend. A gap of ≥4 cm between the diaphragm and the top of the particle bed produces shock velocities similar to experiments with air only, suggesting that shock properties are not sensitive to the gap size. For comparison (Figure 2; dotted dashed line), a pseudogas approximation [*Dobran et al.*, 1993, equations (40) and (41)] underestimates shock velocities and strengths for experiments with particles, where $\alpha = 0.4$, $c_4 = 13$ m s^{-1}, and γ_4 approaches 1 [*Wohletz*, 2001].

[8] Maximum gas-particle mixture velocities occurred in the first 1–12 ms of the experiments, corresponding to accelerations up to 150 g. Mixture velocities increase with increasing pressure ratio and generally decrease with increasing particle size for a given pressure ratio (Figure 3). 1-D shock tube theory using air as an ideal gas significantly overpredicts the mixture velocity and is not plotted. *Cagnoli et al.* [2002] found that a pseudogas approximation is reasonable for mixture velocities with pressure ratios <10 and particle sizes <38 μm. However, our expanded data set shows the pseudogas approximation (Figure 3; dotted dashed line) overpredicts mixture velocities at higher pressure ratios and for larger particles.

5. Interpretation of Results

[9] The initial state of our experiments consists of a packed bed of particles and interstitial air at atmospheric pressure. Upon decompression, the interstitial air rapidly expands, generating a shock wave which propagates faster than the subsequent motion of the air-particle mixture (Figure 1d). Shock strength and velocity are reduced compared to experiments with air only, suggesting that significant drag forces are generated on the air when the expanding gas initially propagates through interstices in the particle bed. A pseudogas approximation underpredicts

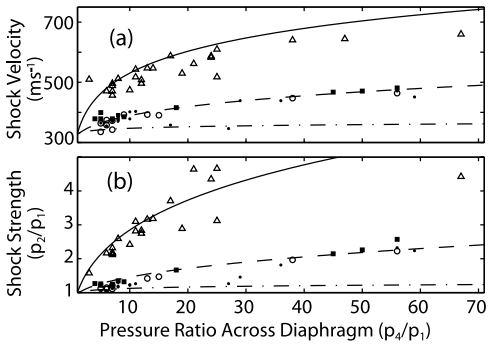

Figure 2. (a) Shock velocity and (b) strength data vs. pressure ratio across the diaphragm (p_4/p_1) for experiments with only air as the driver and expansion gases (open triangles), and experiments with 45 (solid squares), 90 (dots), and 150 μm (open circles) particles. The error for all experimental data is the radius of the plotted symbols. Also shown are 1-D shocktube theory for an ideal gas (solid line), the pseudogas approximation from *Dobran et al.* [1993] (dotted dashed line), and our new model incorporating interphase drag (equations (4) to (7); dashed line).

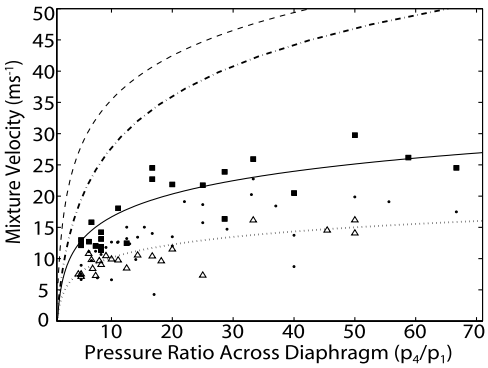

Figure 3. Mixture velocity vs. pressure ratio across the diaphragm (p_4/p_1) for experiments with 45 (solid squares), 90 (dots), and 150 μm (open circles) particles. Error for all experiments is the radius of the plotted symbols. Also shown are the pseudogas approximation of *Dobran et al.* [1993] (dotted dashed line), predictions of the first term of the *Ergun* [1952] equation with 90 μm particles (dashed line), and our new model for 45 μm (solid line) and 150 μm (dotted line) particles.

the shock strength and velocity (Figure 2; dotted dashed line) because experimental observations suggest the shock wave is formed by air, not by an air-particle mixture. Subsequently, the drag of the air generates particle motion. Our experimental results show the velocity of the gas-particle mixture is less than that predicted by pseudogas approximations due to imperfect coupling between particles and air, as has been proposed for large pressure ratios [*Cagnoli et al.*, 2002].

[10] We now estimate the magnitude of the interphase drag forces using two methods. First, we calculate the drag force exerted by the particles on the air by examining air motion across the shock wave, and then we quantify the drag force exerted by the air on the particles by examining the motion of the air-particle mixture.

5.1. Modified Shock Relationship

[11] The drag force exerted by the particles on the expanding air can be introduced into the momentum equation for a control volume (CV1) across the shock wave (Figure 1d) as follows

$$p_2 - p_1 + \frac{F_{da}}{A} = \rho_1 u_1^2 - \rho_2 u_2^2 \tag{3}$$

where F_{da} is the drag force exerted by the particles on the air and A is the cross sectional area of the shock tube occupied by the air ($\propto A_{tube}$, where A_{tube} is the cross-sectional area of the test section), and subscripts 1 and 2 refer to properties of the air in front of and behind the shock, respectively (equation (1); Figure 1; modified from *Saad*, 1985). Equation (3) balances the vertical forces acting on the air in the CV, the net pressure force (first two terms on LHS) and the drag force exerted by the particles (third term on LHS), against the net momentum change across the CV, the difference between momentum entering and leaving the CV (terms on RHS). Rearranging and using the continuity equation for constant A and standard relationships for compressible flow, the modified shock strength can be written as

$$\left(\frac{p_2}{p_1}\right)_{particles} = 1 + \frac{2\gamma}{\gamma+1}\left(M_s^2 - 1\right) - \frac{F_{da}}{Ap_1} \tag{4}$$

[12] Thus, the shock strength formed by gas-particle mixtures is simply that predicted for inviscid flow of an ideal gas alone (equation (1)) reduced by the factor $\frac{F_{da}}{Ap_1}$. In conventional form

$$F_{da} = \frac{1}{2} C_d \rho_2 u_2^2 A \tag{5}$$

where C_d is only a function of particle Reynolds number, NRe. Generally, $C_d = k_1(NRe)^\beta$ for $0.1 < NRe < 10^5$, where values of β for single spheres and beds of spheres fall between 0 and -1.3 [Figure 4; *Batchelor*, 1967; *Ergun*, 1952]. Rewriting the drag term in equation (4)

$$\frac{F_{da}}{Ap_1} = \frac{k_1(NRe)^\beta \frac{1}{2}\rho_2 u_2^2 A}{Ap_1} = k_2 \frac{\rho_2}{\rho_1} u_2^{2+\beta} \tag{6}$$

where $NRe = (\rho_2 u_2 d_p)/\mu_2$, d_p is particle diameter, $p_1 = \rho_1 RT$ (ideal gas), and k_2 is a coefficient that incorporates the remaining terms. The density ratio across the shock for a calorically perfect gas is

$$\frac{\rho_2}{\rho_1} = \frac{1 + \frac{\gamma+1}{\gamma-1}\frac{p_2}{p_1}}{\frac{\gamma+1}{\gamma-1} + \frac{p_2}{p_1}} \tag{7}$$

[*Saad*, 1985]. The trend in our shock data is most closely matched when $k_2 = 7.7 \times 10^{-3}$ and $\beta = -1.2$ (Figure 2; dashed line). A narrow range of acceptable β values falls between -1.25 and -0.9.

5.2. Interphase Drag Relationships

[13] For a second CV bounded at the bottom by the diaphragm and at the top by the point of maximum mixture velocity (~20 cm above the diaphragm; Figure 1d, CV2), the momentum equation in the vertical direction for the gas-particle mixture is given by

$$F_{dp} - F_{gravity} + F_{pressure} = \frac{d}{dt}\int_{CV} u_{mix}\rho_s dV + \int_{CS} u_{mix}\rho_s u_{mix} d\vec{A}_{tube} \tag{8}$$

where F_{dp} is the drag force the air exerts on the particles, t is time, V is volume, CS is the control surface perpendicular to the vertical axis and u_{mix} is the measured mixture velocity. In this form, the momentum equation describes the drag, gravity and pressure forces (terms on LHS) that generate the net momentum change of the mixture across the CV (terms on RHS). We solved equation (8) for F_{dp} and calculated the total drag force of the air on the particles for each experiment. We then used a conventional expression for F_{dp} (e.g., equation (5)) to calculate corresponding C_d's, leading to the following relationship (Figure 4)

$$C_d = k_1(NRe)^\beta. \tag{9}$$

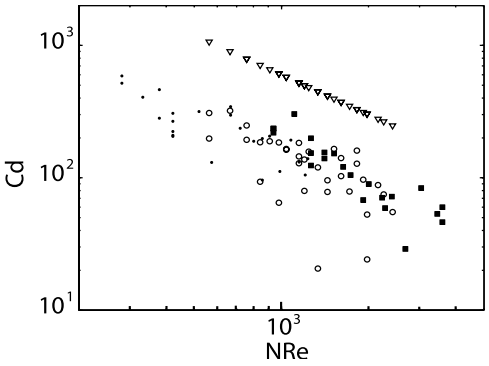

Figure 4. Interphase C_d vs. *NRe* for experiments with 45 (solid squares), 90 (dots), and 150 μm (open circles) particles. The interphase C_d suggested by *Ergun* [1952] for steady flow of air through stationary packed particle beds (90 μm particles; open triangles).

[14] The interphase drag force is controlled by the velocity difference between particles and gas. Because this velocity difference is dominated by air velocity during initial acceleration, u_2 (equation (2)) calculated from the reduced shock strength (equation (4)) is used in *NRe*. Equation (9) follows the functional form for single spheres and beds of spheres identified earlier in the shock analysis, consistent with theory [*Batchelor*, 1967; *Ergun*, 1952]. However, for our experiments ($10^2 < NRe < 10^4$), $k_1 = 7 \times 10^4$ and $\beta = -0.9$ (Figure 4), values which are inconsistent with constants previously obtained for steady-state experiments [*Ergun*, 1952]. According to our experiments, reasonable values of β fall between -1.2 and -0.70, consistent with values obtained from shock observations (section 5.1). Different values of the pre-multiplying constants obtained in the mixture and shock analyses reflect the different stages of particle motion and gas expansion in each case.

[15] The interphase drag relationship suggested by *Ergun* [1952] for steady flow of air through stationary packed particle beds for $NRe < 10$ (first of two terms) can be rewritten as a drag coefficient as follows

$$C_{d,Ergun1} = 5 \times 10^5 (NRe)^{-1} \quad (10)$$

for our experimental conditions. This relationship overpredicts the values of the experimentally determined C_d's by a factor of ~2.5, but the trend parallels our own. The trend for 90 μm particles (open triangles) is shown in Figure 4 for comparison. Use of the Ergun term for NRe > 10 significantly overpredicts our experimental C_d's and is not plotted.

6. Implications for Eruption Dynamics

[16] The gas-particle mixture velocity at the vent is a critical parameter that determines whether pyroclastic flows will subsequently develop [*Sparks et al.*, 1978; *Wilson et al.*, 1980]. Thus, a method of predicting initial explosion velocity for a given conduit pressure is valuable. Conversely, accurately describing the relationship between conduit pressure and explosion velocity and shock wave characteristics provides an estimate of pre-eruption conduit pressures from field observations.

[17] Shallow conduit overpressures on the order of 5–10 MPa precede Vulcanian eruptions, corresponding to initial pressure ratios of 50–100 [*Stix et al.*, 1997; *Voight et al.*, 1999]. For initial $\alpha = 0.4$ and pressures in this range, our experimental data suggest that instantaneous decompression generates mixture velocities of 15–40 m s^{-1}, whereas a pseudogas approximation predicts velocities up to four times greater, and the drag coefficient as described by *Ergun* [1952] predicts mixture velocities up to two times greater. We expect higher experimental mixture velocities for $\alpha > 0.4$ for the same pressure range.

[18] Six Vulcanian eruptions during 1982–1983 at Sakurajima volcano, Japan, had explosion (mixture) velocities of 21–33 m s^{-1} and shock velocities of 440–500 m s^{-1} [*Ishihara*, 1985]. Our analysis of these explosion velocities suggests pre-eruption conduit pressures of 1.5–10 MPa, compared to conduit pressures of 0.4–1.2 MPa estimated using pseudogas theory. Similarly, Vulcanian eruptions during 2002–2004 at Santiaguito volcano, Guatemala, had explosion velocities of 5–30 ms^{-1} [*Bluth and Rose*, 2004] with our theory suggesting initial pressure ratios of 5–100. Our analysis of Sakurajima shock velocities produces conduit pressures of 4–7.5 MPa consistent with the mixture velocity estimates, whereas assuming inviscid flow of an ideal gas suggests conduit pressures of 0.6–1.0 MPa. Given overpressures typically associated with Vulcanian eruptions (5–10 MPa) and the rupture strength of many volcanic rocks (>4 MPa [*Stix et al.*, 1997; *Voight et al.*, 1999]), pseudogas and inviscid shock theories appear to significantly underestimate pre-eruption conduit pressures.

7. Conclusions

[19] Shock strength and velocity are reduced for rapid decompression of solid-gas mixtures as compared to decompression of an ideal gas alone ($10^2 < NRe < 10^4$; $1 < p_4/p_1 < 70$). The magnitude of the reduction is independent of particle size and can be expressed as a simple function of gas properties (equation (6)). Pseudogas theory underpredicts both the shock strength and velocity, and overpredicts maximum gas-particle mixture velocities, which decrease with increasing particle diameter for a given initial pressure ratio. Expressions used previously to describe drag between gas and particles do not correctly predict the maximum mixture velocities observed in our experiments. We therefore present new predictions for shock strength and velocity for gas-particle mixtures (equations (4) to (7)), which are in accord with experimental observations, and develop an improved interphase drag relationship for the eruption initiation stage (equation (9)).

[20] **Acknowledgments.** This research was supported by the Royal Society of London and NSF EAR0541925. Insightful comments from an anonymous reviewer improved the manuscript.

References

Anilkumar, A. V., R. S. J. Sparks, and B. Sturtevant (1993), Geological implications and applications of high-velocity two-phase flow experiments, *J. Volcanol. Geotherm. Res.*, *56*, 145–160.

Batchelor, G. K. (1967), *An Introduction to Fluid Dynamics*, 1st ed., 615 pp., Cambridge Univ. Press, New York.

Bluth, G. J. S., and W. I. Rose (2004), Observations of eruptive activity at Santiaguito volcano, Guatemala, *J. Volcanol. Geotherm. Res.*, *136*, 297–302.

Cagnoli, B., A. Barmin, O. Melnik, and R. S. J. Sparks (2002), Depressurization of fine powders in a shock tube and dynamics of fragmented magma in volcanic conduits, *Earth Planet. Sci. Lett.*, *204*, 101–113.

Dobran, F., A. Neri, and G. Macedonio (1993), Numerical simulations of collapsing volcanic columns, *J. Geophys. Res.*, *98*, 4231–4259.

Ergun, S. (1952), Fluid flow through packed columns, *Chem. Eng. Prog.*, *48*, 89–94.

Ishihara, K. (1985), Dynamical analysis of volcanic explosion, *J. Geodyn.*, *3*, 327–349.

Johnson, J. B., R. C. Aster, M. C. Ruiz, S. D. Malone, P. J. McChesney, J. M. Lees, and P. R. Kyle (2003), Interpretation and utility of infrasonic records from erupting volcanoes, *J. Volcanol. Geotherm. Res.*, *121*, 15–63.

Kieffer, S. W. (1981), Fluid dynamics of the May 18 blast at Mount St. Helens, *U.S. Geol. Surv. Prof. Pap.*, *1250*, 379–400.

Melnik, O., A. A. Barmin, and R. S. J. Sparks (2005), Dynamics of magma flow inside volcanic conduits with bubble overpressure buildup and gas loss through permeable magma, *J. Volcanol. Geotherm. Res.*, *143*, 53–68.

Morrissey, M. M., and B. A. Chouet (1997), Burst conditions of explosive volcanic eruptions recorded on microbarographs, *Science*, *275*, 1290–1293.

Neri, A., and G. Macedonio (1996), Numerical simulation of collapsing volcanic columns with particles of two sizes, *J. Geophys. Res.*, *101*, 8153–8174.

Saad, M. A. (1985), *Compressible Fluid Flow*, Prentice-Hall, Upper Saddle River, N. J.

Sparks, R. S. J., L. Wilson, and G. Hulme (1978), Theoretical modeling of the generation, movement, and emplacement of pyroclastic flows by column collapse, *J. Geophys. Res.*, *83*, 1727–1739.

Stix, J., R. C. Torres, L. Narvez M, G. P. Corts J, J. A. Raigosa, D. Gmez M, and R. Castonguay (1997), A model of Vulcanian eruptions at Galeras volcano, Colombia, *J. Volcanol. Geotherm. Res.*, *77*, 285–303.

Valentine, G. A., and K. H. Wolhletz (1989), Numerical models of Plinian eruption columns and pyroclastic flows, *J. Geophys. Res.*, *94*, 1867–1887.

Voight, B., R. S. J. Sparks, A. D. Miller, R. C. Stewart, R. P. Hoblitt, A. B. Clarke, J. Ewart, and MVO Staff (1999), Magma flow instability and cyclic activity at Soufrire Hills Volcano, Montserrat, *Science*, *283*, 1138–1142.

Wallis, G. B. (1969), *One-Dimensional Two-Phase Flow*, McGraw-Hill, New York.

Wilson, L., R. S. J. Sparks, and G. P. L. Walker (1980), Explosive volcanic eruptions IV. The control of magma properties and conduit geometry on eruption column behaviour, *Geophys. J. R. Astron. Soc.*, *63*, 117–148.

Wohletz, K. H. (2001), Pyroclastic surges and compressible two-phase flow, in *From Magma to Tephra*, edited by A. Freundt and M. Rosi, pp. 247–312, Elsevier, New York.

K. Chojnicki and A. B. Clarke, School of Earth and Space Exploration, Arizona State University, Box 871404, Tempe, AZ 85287–1404, USA. (kirsten.chojnicki@asu.edu; amanda.clarke@asu.edu)

J. C. Phillips, Centre for Environmental and Geophysical Flows, Department of Earth Sciences, University of Bristol, Queens Road, Bristol BS8 1RJ, UK. (j.c.phillips@bristol.ac.uk)